NeuroImage 230 (2021) 117806

Contents lists available at ScienceDirect

NeuroImage

journal homepage: www.elsevier.com/locate/neuroimage

Assessing the effective connectivity of premotor areas during real vs imagined grasping: a DCM-PEB approach

Federica Bencivenga [a,b,c,*], Valentina Sulpizio [a,c], Maria Giulia Tullo [a,b,c], Gaspare Galati [a,c]

[a] Brain Imaging Laboratory, Department of Psychology, Sapienza University, Rome, Italy
[b] PhD program in Behavioral Neuroscience, Sapienza University, Rome, Italy
[c] Cognitive and Motor Rehabilitation and Neuroimaging Unit, Santa Lucia Foundation (IRCCS Fondazione Santa Lucia), Rome, Italy

ARTICLE INFO

Keywords:
Grasping network
Motor imagery
fMRI
Dynamic causal modelling
Parametrical empirical bayes
Supplementary motor area

ABSTRACT

The parieto-frontal circuit underlying grasping, which requires the serial involvement of the anterior intraparietal area (aIPs) and the ventral premotor cortex (PMv), has been recently extended enlightening the role of the dorsal premotor cortex (PMd). The supplementary motor area (SMA) has been also suggested to encode grip force for grasping actions; furthermore, both PMd and SMA are known to play a crucial role in motor imagery. Here, we aimed at assessing the dynamic couplings between left aIPs, PMv, PMd, SMA and primary motor cortex (M1) by comparing executed and imagined right-hand grasping, using Dynamic Causal Modelling (DCM) and Parametrical Empirical Bayes (PEB) analyses. 24 subjects underwent an fMRI exam (3T) during which they were asked to perform or imagine a grasping movement visually cued by photographs of commonly used objects. We tested whether the two conditions a) exert a modulatory effect on both forward and feedback couplings among our areas of interest, and b) differ in terms of strength and sign of these parameters. Results of the real condition confirmed the serial involvement of aIPs, PMv and M1. PMv also exerted a positive influence on PMd and SMA, but received an inhibitory feedback only from PMd. Our results suggest that a general motor program for grasping is planned by the aIPs-PMv circuit; then, PMd and SMA encode high-level features of the movement. During imagery, the connection strength from aIPs to PMv was weaker and the information flow stopped in PMv; thus, a less complex motor program was planned. Moreover, results suggest that SMA and PMd cooperate to prevent motor execution. In conclusion, the comparison between execution and imagery reveals that during grasping premotor areas dynamically interplay in different ways, depending on task demands.

1. Introduction

The neural mechanisms underlying planning and executing a grasping movement, according to the visual features of an object, are still debated. Pioneer studies (Jeannerod et al., 1995; Fagg and Arbib, 1998; Rizzolatti and Luppino, 2001; Arbib and Mundhenk, 2005) enlightened the role of the "visuo-motor grasping circuit", which in macaques includes the anterior intraparietal area (AIP) and the ventral premotor cortex that corresponds to the cytoarchitectonically and functionally non-homogenous area F5 (Belmalih et al., 2009; Gerbella et al., 2011; Sharma et al., 2019; for a review, see Gerbella et al., 2017). According to these models, both areas seem to encode the goal of the action (Fogassi et al., 2001; Castiello and Begliomini, 2008) as well as the grip component of grasping, leading to the correct shape of the hand. Indeed, AIP encodes a 3D representation of the object to grasp and its affordances, while F5 stores a "vocabulary" where the action goals and the postures for grasping are represented, in order to select the most appropriate one according to the features of the object (for reviews, see Castiello and Begliomini, 2008; Gerbella et al., 2017). A collection of positron emission tomography (PET), functional magnetic resonance imaging (fMRI) and transcranial magnetic stimulation (TMS) studies has identified human homologues of these areas based on their similar functional and anatomical arrangement (Grafton et al., 1996; Faillenot et al., 1997; Binkofski et al., 1998; Culham et al., 2003; Culham 2004; Frey et al., 2005; Davare et al., 2006, 2007; Begliomini et al., 2007b; Dafotakis et al., 2008; for reviews, see also Davare et al., 2011; Gerbella et al., 2017). It has been proposed that some functional properties of these areas are shared across species. For instance, most neurons in AIP encode the object shape and, to a lesser extent, its size (Schaffelhofer and Scherberger, 2016); also in humans it has been proved that aIPs encodes intrinsic properties of the objects, such as their size, and not their extrinsic properties such as location (Monaco et al., 2015). Similarly, inactivation of both F5 (Fogassi et al., 2001) and PMv (Davare et al., 2006) results in an alteration of the grip but not of the transport component of grasping.

* Corresponding author.
E-mail address: bencivenga.federica@gmail.com (F. Bencivenga).

https://doi.org/10.1016/j.neuroimage.2021.117806
Received 29 October 2020; Received in revised form 20 January 2021; Accepted 23 January 2021
Available online 29 January 2021

Following studies have suggested an extension of the macaque AIP-F5 circuit, focusing on the role of the dorsal premotor cortex (F2), traditionally known to be involved in reaching. Raos et al. (2004) demonstrated that this area is not only involved in the transport component of grasping, but also has a key role in keeping the motor representation of the object in memory and in updating hand movements (especially the configuration of fingers) as the hand approaches the object. Accordingly, it has been shown that some neurons in F2 are only tuned to reaching, others only to grasping, and others to both (Cao et al., 2013). More recently, a similar role of PMd during grasping has been found in humans by a wide range of studies using different techniques (Davare et al., 2006; Begliomini et al., 2007a; Nowak et al., 2009; Cavina-Pratesi et al., 2010; Gallivan et al., 2011b; Fabbri et al., 2016; Turella et al., 2020).

Castiello and Begliomini (2008) suggested that the areas of the grasping circuit are serially activated, since the information appears to flow from aIPs to PMv, then to PMd, and finally to M1 (F1 in macaques). The primary motor cortex is activated even prior to movement execution and is likely responsible for the motor output through the corticospinal tracts (CST) (Muakkassa & Strick 1979; Godschalk et al., 1984; Matelli et al., 1986; Dancause et al., 2006), besides contributing to the internal prediction of the consequences of the movement (Seki and Fetz, 2012; Sun et al., 2015). A serial involvement of areas of the grasping circuit is also suggested by a series of human neurostimulation studies on precision grasping: whereas aIPs encodes for the visual representation of the object 270–220 ms before the fingers touch the object (Davare et al., 2007), PMv activates about 50 ms later (Davare et al., 2006). Finally, PMd activates around ~100 ms after the PMv (Davare et al., 2006).

Even if the supplementary motor area (SMA, F3 in macaques) was traditionally considered to be involved in the generation of internally driven complex movements (Orgogozo and Larsen, 1979; Roland et al., 1980; Goldberg, 1985), more recent studies have demonstrated an involvement of SMA in sequence planning (for a review, see Cona and Semenza, 2017) and visually guided movements such as reaching (Picard and Strick, 2003). Although SMA is not included in the grasping circuit, there is evidence that it might be involved in encoding some aspects of grasping movements, such as grip force scaling (Smith et al., 1981; Kuhtz-Buschbeck et al., 2001; Haller et al., 2009; White et al., 2013). Grip force is a crucial feature in grasping, since it must be modulated to grasp the object firmly, but without damaging it or let it slip (Johansson and Westling, 1984, 1988).

Dynamic Causal Modelling (DCM; Friston et al., 2003) is a framework for effective connectivity which allows testing hypotheses on the couplings among areas both in resting state (Friston et al., 2014) and during the execution of a task. Previous studies have applied DCM to fMRI data acquired during the execution of grasping; for instance, it has been proved that the dorsolateral (aIPs and PMv) and the dorsomedial (V6A and PMd) parieto-frontal circuits are differently modulated by grasping small or large objects (Grol et al., 2007). A DCM study by Begliomini et al. (2015) has shown that during a reach-to-grasp movement there is an increase in effective connectivity from aIPs to PMv, and from PMv to PMd. However, these studies did not explore the contribution of SMA in grasping; furthermore, they did not use commonly used objects, but manipulanda or boxes instead.

An attractive chance to disclose the underpinnings of motor processes is offered by the comparison between motor execution (ME) and imagery (MI). These two modalities recruit partially overlapping circuits: on the one hand, both seem to rely on a similar processing of motor temporal and spatial information, implemented by associative and premotor brain areas; on the other hand, it is still debated whether they share activity in M1 (for meta-analytic reviews, see Hètu et al., 2013; Hardwick et al. 2018; Papitto et al., 2020). However, striking evidences suggest that univariate fMRI analysis may not exhaustively account for eventual similarities or differences between these two modalities. By taking advantage of multivoxel pattern analysis (MVPA; Edelman et al., 1998; Haxby et al., 2001), it has been revealed that during motor tasks the main motor-related areas, included M1, encode the content of MI (Pilgramm et al., 2016) and that the overall neural representation of MI is similar but still distinct relative to ME (Zabicki et al., 2017; Monaco et al., 2020). By employing the multivariate Bayes (MVB) method (Friston et al., 2008), Park et al. (2015) found that movements were best predicted by M1 during ME, and by SMA during MI. An additional contribution potentially able to disentangle the neural substrates of ME and MI comes from effective connectivity approaches. In this vein, previous studies have clarified that during motor tasks the coupling between SMA and M1 is differently modulated by ME and MI (Solodkin et al., 2004; Kasess et al., 2008; Gao et al., 2011, 2014), e.g., during ME SMA exerted a positive influence on M1, whereas during MI the modulation on M1 became suppressive. These findings, combined with the above-mentioned MVPA studies, point toward the view that a similar, though not equal, implementation of the motor program is required during ME and MI and that, crucially, additional processes may take place during imagery to prevent the actual execution of the movement. However, the above-mentioned effective connectivity studies used imagery in low-demanding tasks (i.e., finger tapping).

Here, we provide the first attempt to apply DCM to imagery of a grasping movement by re-analysing previously collected fMRI data relative to execution and imagery of a pantomimed grasping of commonly used objects (Sulpizio et al., 2020). Several studies have pointed toward a neural similarity between pantomimed and actual movements (Choi et al., 2001; Binkofski and Buxbaum, 2013). During grasping, slight differences in the activity of aIPs were found across pantomime and actual motor execution (Hermsdörfer et al. 2007; Króliczak et al., 2007), presumably due to differences in the perceived goal of the action rather than in the motor planning *per se*. Notice that here we used pantomimed grasping to focus on the motor dynamics that finely regulate the planning and the execution of grasping, avoiding spurious contamination of the signal deriving from hand-object interactions. In the original study, we found a wide network of frontoparietal regions, such as aIPs, PMv, PMd and SMA, which are commonly activated by both imagery and execution of grasping coherently with the view of a similar recruitment of motor-related areas across modalities. In this vein, in the present study we sought to disentangle the direct and the modulatory effects of two exogenous variables (i.e., executed and imagined grasping) on a large motor network, including SMA. Accordingly, we used the computationally efficient Parametrical Empirical Bayes (PEB) approach recently introduced by Friston et al. (2015, 2016) to test both the feedback and the forward connections within our network of interest; by doing so, we hypothesized that we could get new insights on the involvement and the functional role of the key areas involved in grasping. Furthermore, we hypothesized that grasping execution and imagery would require a different involvement of premotor areas; thus, we expected the two conditions to differently modulate the effective connectivity among the key areas involved in grasping, in terms of the sign of the parameters (e.g., a connection would be positively modulated by grasping execution, and negatively modulated by imagined grasping) and of the connection strengths (e.g., reduced values of parameters in imagery relative to motor execution).

2. Methods

2.1. Participants

The present study is based on a reanalysis of BOLD data from a sample of twenty-five healthy subjects (22 females, mean age 26.5, s.d. 3.4) who participated to a previous study from our lab (Sulpizio et al., 2020). All participants were right-handed, as assessed by the Edinburgh Handedness Inventory (Oldfield, 1971), had normal or corrected-to-normal vision, and gave their written informed consent to participate. The study was approved by the local research ethics committee of the IRCCS Fondazione Santa Lucia in Rome, according to the Declaration of Helsinki.

2.2. Procedure and experimental design

The experimental design is fully described in Sulpizio et al. (2020). Participants underwent an fMRI exam during which they were asked to execute a pantomimed grasping ("real" condition) or imagine the same movement ("imagined" condition). In both conditions, subjects saw the picture of an object, randomly chosen from a set of 36 black-and-white photographs of commonly used objects; in the "real" condition, participants were instructed to move the fingers and the wrist of their right hand simulating the grasping of the object, as if it was located in the proximity of their hand. In the "imagined" condition, participants had to imagine and plan the same pattern of movements without actually performing them.

Before entering the scanner, subjects were instructed on the task to perform, accounting for the trial timing and sequence; once in the scanner, they performed a short warm-up phase to familiarize with the setting. During the fMRI exam, an experimenter checked whether during the "real" condition participants moved their hand with the correct timing and according to the instructions, whereas during the "imagined" condition participants remained still.

The experiment used a block design. Each block lasted 16 seconds and was introduced by a written instruction (1 sec) which specified the condition (real or imagined); then, 8 consecutive trials, each lasting 1875 ms, were performed. Each trial started with the presentation in central vision of the graspable object photograph, followed by an inter-trial-interval of 1575 ms during which the subject had to perform or imagine (according to the specified condition) a "whole hand" or a "finger" grasping, depending on the visual stimulus (for more details, see Sulpizio et al., 2020). Graspable object photographs were presented for a very short time (300 ms) to reduce the impact of visual information on BOLD activation. Grasping movements were indeed performed with respect to a "remembered" object not present anymore on the screen. Two runs were performed, each of them composed by 16 experimental blocks (8 for the real pantomimed grasping and 8 for the imagined grasping) plus 4 fixation blocks. Overall, the task consisted of 40 blocks and 256 experimental trials (128 for each condition).

2.2.1. Apparatus

Functional images were acquired at the Neuroimaging Laboratory (Santa Lucia Foundation) using a 3T Siemens Allegra MR system (Siemens Medical systems, Erlangen, Germany) equipped for echo-planar imaging with a standard head coil. Visual stimuli were presented by a control computer located outside the MR room, running in-house software (Galati et al., 2008) implemented in MATLAB (The MathWorks Inc., Natick, MA, USA). An LCD video projector with a customized lens was used to project visual stimuli to a screen placed at the back of the MR tube; participants watched visual stimuli through a mirror positioned inside the head coil. The timing of presentation of each stimulus was controlled and triggered by the acquisition of fMRI images.

We used blood-oxygenation level-dependent imaging (Kwong et al., 1992) to acquire echo-planar functional MR images (TR=2 s, TE=30 ms, flip angle=70°, 64 × 64 image matrix, 3 × 3 mm in-plane resolution, 30 slices, 2.5 mm slice thickness with no gap, ascending excitation order) in the AC–PC plane. Images were acquired starting from the superior convexity and extended ventrally; thus, images included the whole cerebral cortex, but the ventral portion of inferior temporal and occipital gyri. Also, a three-dimensional, high-resolution anatomical image was acquired for each participant (Siemens MPRAGE sequence, TR=2 s, TE=4.38 ms, flip angle=8°, 512 × 512 image matrix, 0.5 × 0.5 mm in-plane resolution, 176 contiguous 1 mm thick sagittal slices). For each scan, we discarded the first four volumes to achieve steady-state, and the experiment started at the beginning of the fifth volume.

Each subject underwent a single acquisition session constituted by two functional scans, each lasting 5'28" (160 functional MR volumes), and one anatomical scan. In order to minimize movements during the scans, subjects' head was stabilized with foam padding and with a chin rest mounted inside the head coil.

2.3. Data analyses

2.3.1. Preprocessing and surface reconstruction

A detailed description of the preprocessing and surface reconstruction steps is provided in our previous paper on the same dataset (Sulpizio et al., 2020). Briefly, we preprocessed and analysed images using SPM12 (Wellcome Department of Cognitive Neurology, London, UK) and FreeSurfer 5.1 (http://surfer.nmr.mgh.harvard.edu/).

We first analysed structural images following the "recon-all" fully automated processing pipeline implemented in FreeSurfer 5.1 (Dale et al., 1999; Fischl et al., 1999a, 1999b; Desikan et al., 2006) in order to obtain a surface representation of each individual cortical hemisphere in a standard space. The surface reconstructions were transformed to the symmetrical FS-LR space (Van Essen et al., 2012) using tools in the Connectome Workbench software (https://www.humanconnectome.org/software/get-connectome-workbench), resulting in surface meshes with approximately 74K nodes per hemisphere.

Functional images were realigned within and across scans to correct for head movement and coregistered with structural MPRAGE scans using SPM12 (Wellcome Department of Cognitive Neurology, London, UK). Functional data were then resampled to the individual cortical surface using ribbon-constrained resampling as implemented in Connectome Workbench (Glasser et al., 2013), and finally smoothed along the surface with an iterative procedure emulating a Gaussian kernel with a 6 mm full width at half-maximum (FWHM).

Then, we analysed functional images for each participant separately on a vertex-by-vertex basis, according to the general linear model (GLM). Neural responses during "active" blocks (the two experimental conditions, "real" and "imagined") were modeled as box-car functions, convolved with a canonical hemodynamic response function and used as separate predictors in the GLM (one for each condition). Passive blocks (fixation) were not explicitly modelled as GLM regressors and were treated as part of the residual variance. As nuisance regressors, we included the framewise displacement (FD), a subject-specific time-series index of the overall estimate of movement over time (Power et al., 2012). We computed FD as the sum of the absolute temporal derivatives of the six head-movement-related parameters (three for translations and three for rotations).

As a final step, we obtained group-level statistical parametric maps by implementing one-sample t tests, comparing signal in each condition relative to the baseline (i.e., real > fixation; imagined > fixation t-contrasts). Statistical maps were obtained with a cluster-forming threshold of $p < 0.001$; we also corrected for multiple comparisons at the cluster level ($p < 0.05$) through a topological false discovery rate procedure (Benjamini and Hochberg, 1995).

2.3.2. Regions of interest selection and time series extraction

Here, we sought to extend our knowledge on the grasping network, adding new light to previous human and monkey studies by providing an estimate of how brain areas interact during grasping movements and their imagination. Although in the GLM analysis reported in Sulpizio et al. (2020) (see also Fig. 1) we observed an extended network of fronto-parietal brain regions involved in both grasping execution and imagery, we focused on a subset of areas basing on theoretical and methodological issues. Firstly, we included areas well known to play a crucial role during grasping (i.e., aIPS, PMv, PMd and M1) and/or during motor imagery (i.e., SMA) according to previous findings and similarly to previous DCM studies on this topic (Kasess et al., 2008; Gao et al., 2011; Begliomini et al., 2015, 2018), also following the model suggested by Castiello and Begliomini (2008). At difference, other brain areas (e.g., the cerebellum, prefrontal areas, V6A) are known to play a

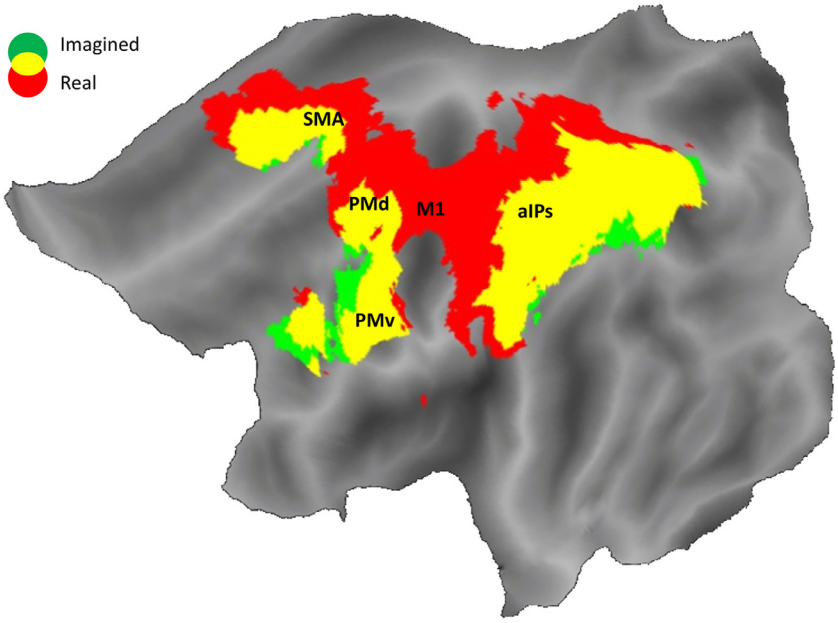

Fig. 1. *Whole-brain results.* Superimposition of the group-activation map associated to the real > fixation t-contrast (in red) and to imagined > fixation t-contrast (in green); commonly activated brain areas are displayed in yellow. The maps are overlaid into the flattened Conte69 atlas (Van Essen et al., 2012) of the left hemisphere. Main activations are labelled as follows: M1, primary motor cortex; aIPs, anterior intraparietal area; PMd, dorsal premotor cortex; PMv, ventral premotor cortex; SMA, supplementary motor area.

role during motor execution (e.g., broad visuomotor processes) or motor imagery but do not peculiarly encode grasping movement properties (Castiello and Begliomini, 2008; Gerbella et al., 2017). Moreover, given that at difference with previous DCM studies we included in the DCM analysis a large number of parameters by modelling reciprocal connections between ROIs (see 2.3.4), focusing on a larger set of ROIs would have further increased the computational load. Thus, we sought to make the DCM analysis computationally more efficient by keeping the model as simple as possible (Stephan et al., 2010). One last issue worth mentioning was that the acquisition sequence prevented the inclusion of occipital and temporal areas, and of the cerebellum as well.

The five ROIs were defined on the cortical surface reconstruction of each individual hemisphere as the regions responding stronger to the real condition than the fixation one (real > fixation t-contrast). Each individual ROI was selected from the resulting statistical map using a threshold-free mapping, by selecting single activation peaks and their neighbourhood (for a maximum of 300 cortical nodes) through a watershed segmentation algorithm as applied to surface meshes (Mangan and Whitaker, 1999). We also used anatomical landmarks as references for the selection of individual ROIs: thus, for instance, M1 was expected to be located near the “hand knob” in the precentral gyrus (Yousry et al., 1997), SMA in the dorsal medial wall, within the interhemispheric fissure, and aIPs at the junction between intraparietal sulcus and postcentral sulcus.

Although the choice of defining ROIs from the real > fixation map may seem biased toward motor execution at the expense of the imagined condition, our choice was motivated by theoretical and technical reasons. First, our group GLM analysis clearly identified a common network across conditions, where almost all the activated areas were recruited more strongly during the real than during the imagined condition (see also Sulpizio et al., 2020). Thus, with the scope of selecting the voxels more representative of the involvement of each region in a grasping task, we considered the real > fixation t-contrast as the most appropriate one, also given that the same criterion was previously adopted in DCM studies when comparing ME and MI (e.g., Kasess et al., 2008). While group-level results suggest that the statistical maps of the imagined condition are to a lesser extent representative of the recruitment of the areas of the grasping network, technical reasons led us to reject the possibility to use the conjunction map between execution and imagery. Indeed, a conjunction map is computed as the voxel-by-voxel minimum between the statistical maps of different conditions, in our case the two conditions relative to the fixation. Given that the activations in the imagery task were overall locally lower than the activations in the “real” task, the conjunction map would have been nearly identical to the motor imagery contrast map, thus yielding to an inappropriate selection of the ROIs. A last worth mentioning technical consideration was that the watershed algorithm we applied to segment the individual activation maps uses the intrinsic spatial gradient of the contrast map, which is partially disrupted by taking at each point the minimum of two maps as happens when using conjunction maps. Not lastly, only during the real condition we found a reliable activation of M1, thus making other possible mapping criteria (i.e., imagined > fixation t-contrast; real > fixation & imagined > fixation conjunction analysis) unsuitable for the primary motor cortex. Consequently, only selecting ROIs from the real > fixation t-contrast would have allowed us to map all the ROIs from the same statistical map.

For each subject and region, we extracted “adjusted” time series from individual surface ROIs, i.e., after regressing out effects of no interest. To carry out the DCM analysis, a single representative timeseries was computed for each ROI retaining the first principal component (eigenvariate) of adjusted data.

2.3.3. *Dynamic causal modelling*

To evaluate the modulation exerted by real and imagined grasping on the effective connectivity between the selected ROIs, we used Dynamic Causal Modelling (DCM) (Friston et al., 2003), implemented in SPM12 (r7771). We hypothesized that both conditions would exert a modulation on all the connections of our model, but that the two conditions would differ in terms of strength and sign of the parameters representing each modulated connection. For instance, we supposed that the parameter representing a specific connection in the “real” condition might have a higher value or a different sign respect to the parameter of the “imagined” condition for the same connection. Coherently with previous effective connectivity studies on MI and ME (Solodkin et al., 2004; Kasess et al., 2008; Gao et al., 2011, 2014), we also expected to find imagery-specific negative modulations that may account for actual movement inhibition.

Briefly, DCM uses an extended balloon model (Buxton et al., 1998; Friston et al., 2000) that explains neuronal dynamics through bilinear approximations. The following equation expresses the neuronal model

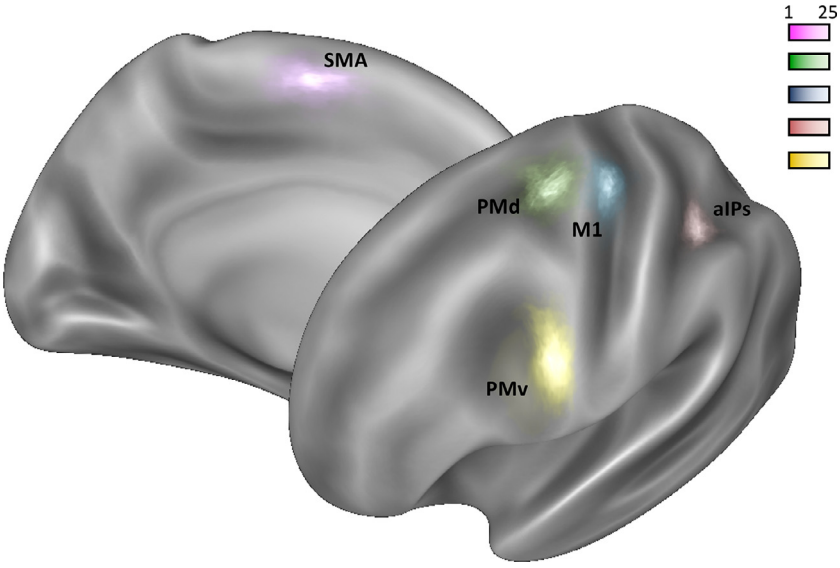

Fig. 2. *Anatomical location of regions of interest (ROIs).* The ventral premotor area (PMv) is shown in pale yellow, the dorsal premotor area (PMd) in pale green, the primary motor cortex (M1) in blue, the anterior intraparietal area (aIPs) in pink, and the supplementary motor area (SMA) in purple. Probabilistic ROIs are overlapped onto an inflated Conte69 brain atlas (left hemisphere) in different views (dorsolateral and medial). The color scale represents the proportion of subjects whose ROI included that node: the lighter the color (i.e., close to white), the higher the probability that the node is common across the 25 individual ROIs.

that allows evaluating the changes in neuronal states over time:

$$\dot{z} = \left(A + \sum_{j=1}^{M} u_j B^j\right) z + Cu$$

where $\dot{z}$ is the derivative of the hidden neural state for each region, and u represents the experimental inputs (Dijkstra et al., 2017). The A matrix stands for the intrinsic coupling between nodes; the B matrix represents the modulatory effect exerted by specific inputs on the connectivity between nodes; the C matrix encodes the direct effect of a driving input on the hidden neural states.

2.3.4. Specification of the model: driving inputs and modulation of connectivity

DCM requires an a priori specification of a biologically and anatomically plausible model which explains how regions of interest interact; basing on this model, connectivity parameters are estimated. In the A matrix, our model included endogenous connections which have been reliably identified in anatomical studies in macaques (for a review, see Davare et al., 2011; for a detailed list of the considered monkey studies, see Supplementary Table 1). Note that, since anatomical studies have not proved the existence of reciprocal connections between aIPs and M1, PMd and SMA, these parameters were switched off (setting their prior expectation to zero and their variance close to 0). Furthermore, we did not centre the input; therefore, in our model the A matrix represents the unmodelled baseline connectivity, in absence of external stimulation (Zeidman et al., 2019a).

In our model, the B matrix consisted of all the possible modulatory effects of each condition on the exogenous connections modelled in the A matrix, except for the feedback exerted by M1 to the other areas. Indeed, differently from previous DCM studies (Begliomini et al., 2015, 2018), we decided to include in the B matrix not only forward connections, but also the feedback ones in order to have a more complete view of how these areas interact during grasping.

In our task, the execution and the imagination of grasping are driven by a visual stimulus; however, since we were not interested in modeling the visual processing of the stimulus, we modelled both inputs (grasping execution and imagination) to exert a direct effect only on aIPs. Indeed, according to the model described by Castiello and Begliomini (2008) and to the DCM analysis performed by Begliomini et al. (2015, 2018), the visuomotor analysis of the to-be-grasped object is supposed to start from aIPs. Furthermore, TMS studies have supported this hypothesis showing that aIPs is involved in grasping ~50-100 ms before the premotor areas (Davare et al., 2006, 2007). The driven inputs of imagined and real conditions on aIPs stand for the C matrix.

2.3.5. Estimation of DCM and parametrical empirical Bayes (PEB)

To compare the changes in connectivity caused by the task, separately in the real and in the imagined condition, we used a DCM-PEB approach. Parametrical Empirical Bayes (PEB) (Friston et al., 2015, 2016) is a hierarchical Bayesian model that uses both non-linear (at first level) and linear (at second level) analyses. The main advantage of using PEB is to assess commonalities and differences among subjects in the effective connectivity domain at the group level and, thus, taking into account the variability in individual connections strength, i.e., the uncertainty over parameters represented by their covariance matrix. By doing so, this approach reduces the weight of subjects with noisy data (Zeidman et al., 2019b). In our study, we used the most recent PEB approach since we had specific hypotheses regarding the anatomical constraints of our model but not the direction and the strength of our parameters, especially in the imagined condition.

Time series extracted from individual ROIs were carried into DCM analysis for the first level, in which a fully connected model (with previously hypothesized constraints) was estimated for each subject. The inversion (estimation) of the model uses the Variatonal Laplace estimation scheme (Friston et al., 2007), which allows finding the predicted time series that matches the observed time series as much as possible, minimizing movement of the parameters from their prior values. By doing so, the score of the quality of the model, i.e., the (negative) variational free energy, may be maximized finding the neural parameters which offer the best trade-off between model accuracy and complexity.

Before computing the analyses at the group level, we checked that for each subject the variance explained by the model was at least of 10%, as an index of the success of model inversion (Zeidman et al., 2019a); one subject did not respect this constraint and was excluded from further analyses. Then, we collapsed DCMs from the remaining 24 subjects in order to perform PEB second level (between subjects) analysis over the first-level DCM parameter estimates. We chose to carry out separate PEB analyses, one for the A matrix and another one for B and C matrices. Indeed, since our analysis involved a large number of parameters, we wanted to avoid dilution of evidence effect, reducing the search space (Zeidman et al., 2019b). Furthermore, since we were interested only in the group means, we did not model other between-subjects effects. As a consequence, we used a between-subject design matrix $X = [1 \ldots 1]^T$.

Having estimated the full model (with all connections of interest switched on) for each subject, the PEB approach requires to perform

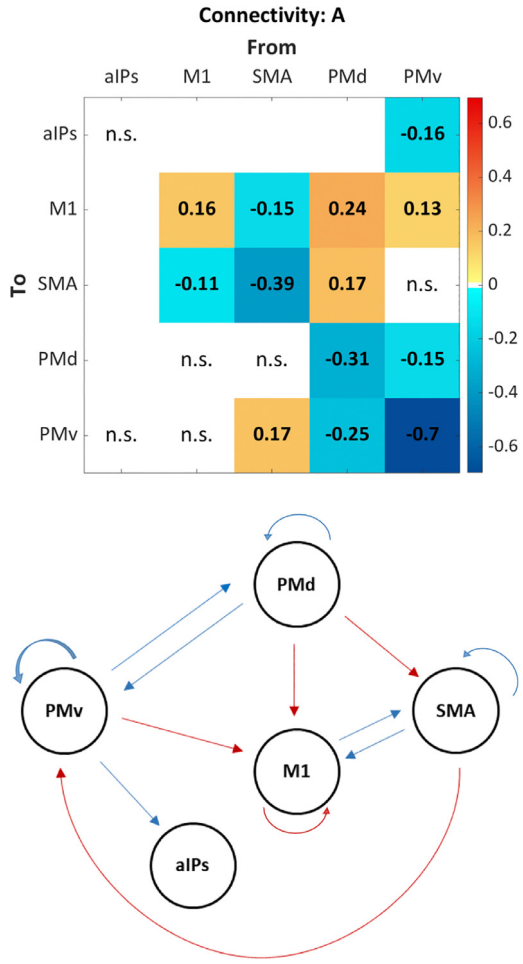

Fig. 3. *PEB results – A matrix.* The left side of the figure shows the matrix of the effective connectivity of the unmodelled baseline; only suprathreshold parameters (posterior probability > 0.95) are shown, whereas subthreshold parameters are marked with "n.s." (i.e., non-suprathreshold), and non modelled connections, i.e, whose priors are set to 0, are displayed in white. Connection strengths are represented in a scale from yellow to dark red, if excitatory, and from turquoise to dark blue, if inhibitory. Values of connection strengths are also provided. The right side of the figure also shows a schematic representation of the corresponding matrix, displaying only suprathreshold connections: line thickness reflects the strength of the respective connection; red lines denote excitatory connections, blue lines stand for inhibitory connections.

Bayesian model reduction (BMR) and Bayesian model Average (BMA).

Briefly, BMR is a particularly efficient form of Bayesian model selection (BMS) that, using a greedy search, automatically compares the full model with 256 models where one or more connections, which have the least evidence, are pruned out and thus switched off, whereas the parameters with the most evidence are kept stable (Friston and Penny, 2011; Friston et al., 2016; Pinotsis et al., 2016). Indeed, each reduced model has a probability density over the possible values of parameters (connection strengths) that maximizes the score for the quality of the model (Zeidman et al., 2019a).

We performed BMA analysis to average the parameters across models, weighted by the evidence of each model (Hoeting et al., 1999; Penny et al., 2006; Rosa et al., 2012).

Finally, we used a threshold based on free energy, taking into account the covariance of parameters, to evaluate whether a parameter contributed to the model evidence. We selected parameters keeping only those with strong evidence, i.e., posterior probability > 0.95; this value represents the probability of the parameters of being present vs absent.

In order to compare the strength in effective coupling between the two conditions, we computed Bayesian contrasts (Dijkstra et al., 2017) over the parameters of the B matrix that exceeded the threshold. After having computed the posterior mean (m), variance (v) and probability of the contrast, we evaluated the posterior distribution over it. This procedure allowed us to take into account the uncertainty of the estimated parameters.

Table 1
Mean peak coordinates and standard deviations of individual ROIs.

Region	MNI Coordinates		
	x	*y*	*z*
aIPs	-37 ± *2,3*	-40 ± *2,9*	42 ± *3,2*
M1	-35 ± *3,3*	-22 ± *4,2*	57 ± *5,9*
SMA	-5 ± *1,2*	-5 ± *5,2*	58 ± *3,2*
PMd	-26 ± *3,8*	-11 ± *2,2*	54 ± *5,7*
PMv	-50 ± *4,1*	5 ± *2,4*	31 ± *5,5*

3. Results

3.1. Whole-brain analysis and ROIs selection

A detailed description of the whole-brain GLM analysis is provided in our previous study on the same dataset (Sulpizio et al., 2020). Fig. 1 shows an overlap of the group activation maps, as resulting from the two conditions, overlaid onto the flattened atlas Conte69. Since the present study focuses on the contralateral hemisphere to the moving hand, only results in the left hemisphere are shown.

In both the real > fixation and the imagined > fixation t-contrast a wide frontoparietal network emerged. Frontal activations encompassed premotor areas (e.g., PMd, PMv) and, in the dorsal medial wall, an activation of SMA emerged. The parietal activations included the posterior intraparietal sulcus (pIPs), with the adjoining superior (SPL) and inferior (IPL) parietal lobules, and the supramarginal gyri (sMg). In this territory, we found a strong focus of activation in aIPs.

Notably, at difference with the imagined condition, during pantomimed grasping the frontal activation encompassed the hand territory of the left primary motor and somatosensory areas (M1 and S1).

To perform the following DCM analysis, we selected for each subject the regions of interest from the individual cortical surface, inspecting the real > fixation statistical map. The activation plots of the ROIs across the two conditions are provided in the Supplementary Figure 1.

To provide a visual representation of the anatomical location of the ROIs, we combined them across subjects to create probabilistic maps. Fig. 2 shows the probabilistic ROIs overlaid onto the inflated Conte69 atlas surface (Van Essen et al. 2012). Table 1 also shows mean coordinates of individual ROIs, along with their standard deviations. The location of the probabilistic ROIs resembled the location of the activated foci across both conditions (except for M1).

3.2. DCM analysis

The A matrix represents the baseline connectivity, i.e., the intrinsic coupling between nodes. The leading diagonal of the A matrix (Fig. 3) shows the values of self-connections, which are unitless log scaling parameters scaled up or down the default value of -0.5 Hz (Zeidman et al., 2019a). This means that a positive value stands for an increase in the inhibition of the region, representing its reduced responsivity to the inputs from the network. Our results showed that all the self-connections had negative values, except for M1 and aIPs, even if this parameter did not reach the threshold (connection strength = 0.109, posterior probability = 0.92).

For the other connections, the values resulting from the analysis represent the rate of change, in units of Hz, in the activity of one area ("destination"), caused by the change of the activity in the "source" area. Thus, positive values mean excitatory influences, whereas negative values stand for inhibitory influences. Our results showed that M1 and SMA

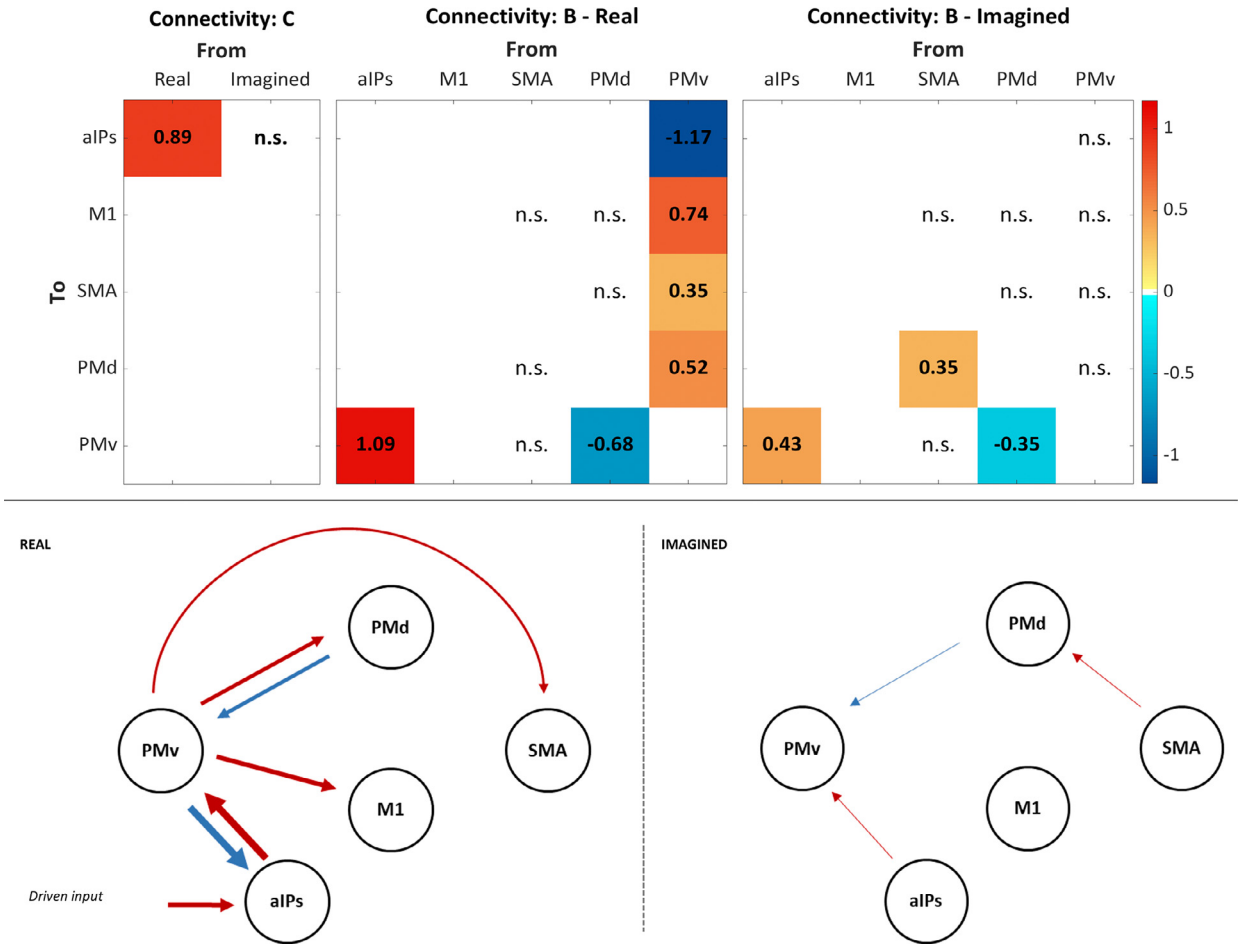

Fig. 4. *PEB results – B and C matrices.* The left side of the top panel shows the matrix of the direct effect exerted by the inputs (i.e., stimuli of the real and the imagined condition) on aIPs; instead, the right side of the top panel shows the matrices of the modulation effect exerted by the conditions on the effective connectivity between regions, separately for the real and the imagined condition. As for Fig. 2, only suprathreshold parameters (posterior probability > 0.95) are shown, whereas subthreshold parameters are marked with "n.s." (i.e., non-suprathreshold), and non modelled connections, i.e., whose priors are set to 0, are displayed in white. Connection strengths are displayed from yellow to dark red (i.e., excitatory), and from turquoise to dark blue (i.e., inhibitory). Values of connection strengths are also provided. The lower panel of the figure also shows a schematic representation of the matrices, separately for the real (left) and the imagined (right) conditions. Only suprathreshold connections are displayed: line thickness reflects the strength of the respective connection; red lines denote excitatory connections, blue lines stand for inhibitory connections.

had a reciprocal negative influence, whereas the connection from SMA to PMv was excitatory. Connections from PMd were excitatory on M1 and SMA, inhibitory on PMv. Finally, PMv had a positive influence on M1, a negative influence on aIPs and PMd.

Fig. 4 shows the results of the B and C matrices. PEB results of the C matrix showed that in the real condition the driven input on aIPs exceeded the threshold of 0.95 and was excitatory, whereas the parameter representing the driven effect of imagery on aIPs did not exceed the threshold.

In the B ("modulatory") matrix, the values resulting from the analysis represent the rate of change, in Hz, in the coupling from an area ("source") to another one ("destination") caused by the experimental input. In the real condition, the major positive modulatory effect of executed grasping propagated from aIPs to PMv, followed by the strong inhibitory feedback exerted by PMv to aIPs. PMv exerted a positive influence on M1, PMd and, to a lesser extent, on SMA. In turn, only PMd had a negative influence on PMv. In the imagined condition, a positive influence from aIPs to PMv and from SMA to PMd emerged; moreover, there was an inhibition of PMv exerted by PMd.

Results of Bayesian contrasts (real > imagined) performed over connections that exceeded the threshold in both conditions are shown in Fig. 5. There was a 100% posterior probability that in the real condition the coupling between aIPs and PMv was higher than in the imagined condition; similarly, inhibition exerted from PMd to PMv was higher in the real than in the imagined condition (posterior probability = 0.96).

4. Discussion

The main aim of our study was to evaluate whether effective connectivity adds some useful insight into the functioning of the visuo-motor grasping circuit, by comparing dynamic couplings during grasping execution and imagery. Our results confirm and extend the knowledge on the functional role of the areas serially involved in grasping.

4.1. Pantomimed grasping

As the classic view of the grasping circuit suggests (Jeannerod et al., 1995), our model confirms that during real grasping the first node involved in the analysis of the stimulus is aIPs (driven input), which has been shown to be activated even during object fixation (Taira et al., 1990; Sakata et al., 1995; Murata et al., 2000).

As emerged from the results of the modulatory matrices, during real grasping all the forward connections among traditional grasping-related areas (aIPs, PMv, PMd, M1) are excitatory (i.e., represented by positive

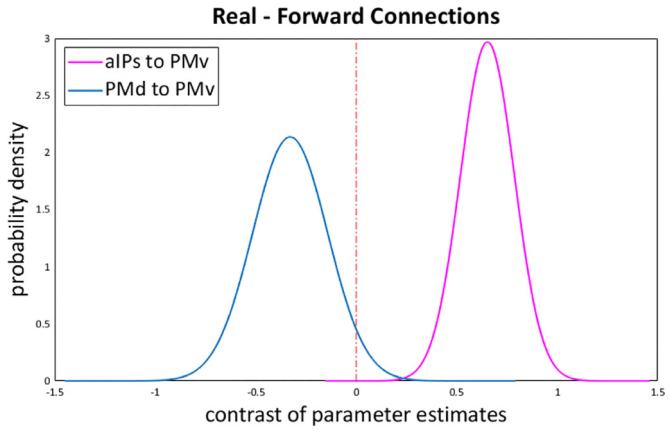

Fig. 5. *Bayesian contrast over parameter estimates (real > imagined).* Plot of the probability density function of the contrast over parameter estimates that exceeded the threshold (posterior probability > 0.95) in both conditions: connection from aIPs to PMv (in purple) and connection from PMd to PMv (in blue). Both contrasts have a posterior probability higher than 0.95 (aIPs to PMv: 1; PMd to PMv: 0.96); thus, both connections are higher in the real than in the imagined condition. However, the direction of the contrast is different among the two connections: the posterior mean of the contrast of the forward connection from aIPs to PMv is positive, i.e., this connection is more excitatory in the real than in the imagined condition; instead, the posterior mean of the contrast of the feedback connection from PMd to PMv is negative, meaning that this connection is more inhibitory in the real than in the imagined condition.

values of posterior estimates); on the contrary, all the feedback couplings are inhibitory. The functional meaning of this evidence might be that the representation stored in the previously activated area is updated based on the new features of the object, processed by the following activated nodes of the circuit. This hypothesis suggests that the role of premotor areas does not run out when the information flows to the following activated areas. Otherwise, the inhibitory feedback couplings might be necessary to downscale the excitation of the previously activated areas. Anyway, both hypotheses support the serial involvement of the areas in the grasping circuit, as suggested not only by the classic models of this circuit but also by human TMS studies (Davare et al., 2006, 2007).

Accordingly, once the network is activated through aIPs, our results show that the visuo-spatial representation of the object is conveyed to PMv to select the motor program (e.g., hand posture) appropriate to the object and to encode the timing of the intrinsic hand muscle recruitment (Olivier et al., 2007). As the next step of the information flow, our results underline the role of PMd and SMA, both receiving an excitatory influence by PMv. Both areas may have a key role in integrating different aspects of the grasping movement, processing low-level features of the movement at high-level processing stages.

Regarding PMd, Fabbri et al. (2016) showed that PMd encodes the number of digits as well as object visual properties. Accordingly, an fMRI adaptation study (Monaco et al., 2015) has shown that while aIPs adapts only to object size, PMd adapts to both object size and location; thus, this area integrates both extrinsic and intrinsic features of the object to plan how to make contact with the object, correctly positioning the fingers. Therefore, it is plausible that PMd updates information previously processed by PMv.

Differently from previous DCM studies, we chose to include SMA in our model, since it seems to be involved in grip force scaling, even if there is no evidence that SMA processes the force *per se* (White et al., 2013). It has been suggested that grip force relies on an internal representation of the object mechanical properties (Flanagan and Wing, 1997) and that, once the most appropriate internal model of the object dynamics has been selected, its implementation might rely on the activity of cerebellum and SMA (Bursztyn et al., 2006; White et al., 2013). Accordingly, our results suggest that the motor program selected by PMv is conveyed to SMA, as this area may be responsible for the integration of the force variation with other features of grasping movement (e.g., timing), at a high-level processing stage (Haller et al., 2009).

The last step of the grasping movement requires the execution of the motor program, which is supposed to be conveyed to the primary motor cortex, responsible for the motor output through the cortico-spinal tracts. Raos et al. (2004) suggested that the connection from F2 to M1 might be responsible for the control of forelimb actions. Thus, contrary to the traditional view which supposes that PMv activates directly M1, Castiello and Begliomini (2008) hypothesized that the connection from PMd to M1 might be the last step of the grasping circuit. However, when these authors tested this network hypothesis with a DCM study (Begliomini et al., 2015), they did not find a significant modulation of grasping on the connection from PMd to M1, while the other connections were significantly modulated by the task (from aIPs to PMv and from PMv to PMd). On the same line, our results showed that M1 receives an excitatory influence only from PMv, and not from PMd; thus, our model supports the classic theories of the visuo-motor grasping circuit (Jeannerod et al., 1995; Fagg and Arbib, 1998; Rizzolatti and Luppino, 2001; Arbib and Mundhenk, 2005).

To sum up, our results support the view of a hierarchical organization of the cortex postulated by Rizzolati et al. (1998), where action representation spans from the abstract encoding of the goals to the concrete representation of motor features (Turella et al., 2020). Indeed, a collection of studies performed with MVPA (Gallivan et al., 2011a, 2011b; Gallivan et al., 2013; Turella et al., 2020) has revealed that goal-related features of actions are encoded by aIPs and PMv, coherently with macaque findings (Fogassi et al., 2001; Castiello and Begliomini, 2008), whereas other areas, as PMd, are responsible for lower-level motor features. Similarly, our findings suggest that planning a grasping movement requires the encoding, in PMv, of a "general" motor program, which is then updated processing low-level motor features of the object (e.g., grip force, wrist orientation, configuration of fingers) that allow grasping it appropriately. These additional features, encoded by SMA and PMd, are not necessary to grasp the object, but allow carrying out a more careful and precise movement.

Since we did not find a direct connection of SMA and PMd to M1, similarly to the finding of Begliomini et al. (2015), it is still unclear how these areas update the motor execution encoding for low-level motor features. Moreover, our results show that, differently from PMd, SMA does not exert a negative feedback on PMv. It has been reported that all premotor areas project to the spinal cord, but in different ways (Dum and Strick, 2005). Indeed, PMv has limited access to motoneurons (Martino and Strick, 1987; He et al., 1993; Shimazu et al., 2004) compared with SMA and PMd. Furthermore, even if PMd projects to the spinal cord, this area does not seem to play a direct role in movement execution, being more involved in action selection (Halsband et al., 1993; Rushworth et al., 1998). Accordingly, our results suggest that PMd sends back an updated motor program to PMv, which in turn conveys it to M1, refining motor execution. Differently, since SMA directly projects to the hand motoneurons (Dum and Strick, 1996; Maier et al., 2002), it may influence the motor execution without conveying the updated motor program to the primary motor cortex through PMv.

4.2. *Imagined vs Pantomimed grasping*

The PEB results of the C matrix did not confirm that imagery exerts a direct effect on aIPs. This result is consistent with studies that have suggested that the activation of aIPs depends on the perceived goal of the action (Fogassi et al., 2001; Hamilton and Grafton, 2006; Króliczak et al., 2007; Tunik et al., 2007). Accordingly, it might be supposed that imagery activates aIPs less than ME in the univariate analysis, and does not exert a direct effect on aIPs in the effective connectivity one, because imagined actions are perceived as less purposeful than executed

pantomimed actions. Furthermore, as stated above, we chose to model the input to have a direct effect only on aIPs, even if both conditions arise from a visual cue; indeed, we were not interested in analysing the visual processing of the stimulus, and the acquisition sequence itself excluded the possibility of modelling occipital areas. However, it has been shown that during imagery there is a major contribution of visual cortices (Guillot et al., 2009; Jiang et al., 2015); therefore, it is unsurprising that during imagery aIPs is not the first involved node in our model.

In the present study, we also aimed at testing the hypothesis that real and imagined grasping would require a different involvement of premotor areas, exploring the difference in couplings between our regions of interest across the two conditions. As expected, our results suggest that during the imagined condition a different connectivity pattern emerges. aIPs exerts a positive influence on PMv, but to a lesser extent than during real grasping; PMv does not exert feedback inhibition on aIPs. A potential explanation of the latter finding may be that during MI the absence of the concrete implementation of the movement prevents the online update of the information stored in aIPs. Indeed, aIPs jointly represents abstract and concrete action properties (Turella et al., 2020) and is known to be involved in online monitoring (Davare et al. 2007; Tunik et al., 2007; Dafotakis et al., 2008), a process that likely takes place thanks to cortico-cortical and cortico-cerebellar loops. This collection of evidence confirms the flexible organization of aIPs that subserves the ability to react to unexpected environmental demands (Turella et al., 2020).

Alongside the aIPs-PMv circuit, the PEB results of the imagined condition show that the motor program appropriate to the object, encoded by PMv, is not conveyed to M1, which is not activated even in our group analysis (Sulpizio et al., 2020), nor to SMA and PMd. Thus, the motor program seems not to be updated by higher-level processing stages encoded by PMd and SMA, suggesting that during imagery a less complex motor program is planned. Despite that, both SMA and PMd seem to play a role during imagery, since SMA activates PMd, which in turn inhibits PMv. It has been proved that both areas are involved during imagery, and that PMd receives inputs from visual areas (Marconi et al., 2001; Simon et al., 2002), even if we did not model these connections. Also, PMd is involved in the selection of the kind of action to be performed (Hoshi and Tanji, 2007). Accordingly, our results suggest that SMA and PMd may cooperate to prevent that the action would be performed, since a crucial input to PMd seems to derive from SMA at difference with executed grasping; this evidence possibly confirms the existence of imagery-specific processes that prevent the execution of the motor plan.

Differently from previous DCM studies on motor imagery during low-demanding tasks such as finger tapping (Kasess et al., 2008; Gao et al., 2014), our model did not show a suppressive influence of SMA on M1. The lower complexity of the movements to be performed, as well as the exclusion of PMd in the above-mentioned DCM studies, may account for the dissimilarity between previous and present DCM results. The study from Park et al. (2015) also points toward this interpretation, since it showed that the predictive role of SMA during imagery differed across tasks (namely, hand grasping and rotation). Moreover, since our results show that M1 is not activated by PMv, and that PMv is inhibited by PMd, one may speculate that during imagined grasping there is no need for SMA to inhibit the primary motor cortex.

The comparison between imagined and real grasping further supports the abstract-to-concrete action representation in the cerebral cortex previously discussed. Indeed, the abstract representation of motor plan during grasping was found to be shared across ME and MI in high-level areas as aIPs (Monaco et al., 2020), and this might explain the cross-condition involvement of the aIPs-PMv circuit in our PEB results. Moreover, PMd was found to represent actions in both ME and MI, irrespective of the complexity of the motor tasks; more intriguingly, this area lacks of generalization across ME and MI during grasping (Monaco et al., 2020), whereas it shows a more similar representation across modalities during low-demanding motor tasks (Zabicki et al., 2017). The above-described and the present findings yield to the suggestion that different, and presumably task-dependent, neural mechanisms take place in PMd. Accordingly, the crucial role of PMd in deciding the kind of action to be performed (Hoshi and Tanji, 2007) may account for differences between MI and ME, and this property may be emphasized when dealing with complex motor movements and their inhibition.

Also the distinct roles of M1 during MI and ME deserve further considerations. The contribution of the primary motor cortex during imagery is controversial, since different techniques and approaches have resulted in contradictory findings. Indeed, some studies have suggested that M1 encodes high-level motor properties such as the goal of the action both in ME and MI (Alexander and Crutcher 1990; Ashe et al., 1993; Gallivan et al., 2011a; Georgopoulos and Grillner, 1989; Kalaska and Crammond, 1992; Pilgramm et al., 2016; Turella et al., 2020), whereas several fMRI activation studies have failed in revealing a consistent contribution of M1 during MI. However, methodological limits (such as the lack of spatial specificity of canonical, volumetric fMRI analyses) may account for eventual null findings; different fMRI techniques, such as MVPA, have indeed suggested that M1 decodes the content of MI (Pilgramm et al., 2016). Of utmost relevance is the usage of high-resolution fMRI (7T) to disentangle the contribution of different layers of the primary motor cortex during MI, compared to ME (Trampel et al., 2019; Persichetti et al., 2020). Monkey (Weiler et al., 2008; Mao et al., 2011) and human (Huber et al., 2017) studies have indeed revealed layer-specific connections of M1, where the superficial layers orchestrate the cortico-cortical connections, whereas the deeper ones are responsible for the generation of cortico-spinal outputs. Accordingly, the usage of the vascular space occupancy (VASO) method that increases the spatial specificity removing the vasculature bias (Turner, 2016; Huber et al., 2018), combined with high-resolution fMRI (7T), revealed that the superficial layers of M1 are recruited during both MI and ME; conversely, the motor outputs are generated in the deeper layers of M1 , but only during ME (Persichetti et al., 2020). Thus, M1 presumably holds, albeit for short periods, high-level motor properties processed by premotor regions. Despite our attempt to increase spatial accuracy by using a surface-based ROIs selection, our analysis may have not reached such degree of specificity.

4.3. Limitations

One limitation of the present study is that we used pantomimed instead of actual grasping. This choice is quite common among fMRI studies due to the difficulty of performing real grasping in the MR environment (Bozzacchi et al., 2012; Johnson-Frey et al., 2005; Makuuchi et al., 2012; Shikata et al., 2003; Simon et al., 2002), especially if the objects to grasp are commonly used objects and not boxes or manipulanda. Moreover, in order to test our hypothesis on motor dynamics during grasping, pantomime allowed us to avoid that hand-object interactions (i.e., touching the object) would result in the activation of sensorial areas, which might superimpose the activation of the motor ones. However, it might be useful to test whether our model is reliable also during actual grasping, despite the tactile stimulation caused by the interaction with the object.

We are aware that grasping execution involves a broader range of areas, for instance prefrontal areas (e.g., dorsolateral and ventrolateral prefrontal cortex) or pre-SMA (F6 in macaques), which interact with motor areas and may play a crucial role in motor dynamics (Gerbella et al., 2017). Similarly, imagery involves also visual (Jiang et al., 2015) and frontal areas such as the dorsolateral prefrontal cortex (Hardwick et al., 2018). Beyond the exclusion of some areas (e.g., cerebellum, occipital and temporal areas) due to the acquisition sequence, we chose not to include other areas in our model to focus on brain regions known to peculiarly encode grasping movement proper-

ties; furthermore, this allowed us to keep the DCM model as simple as possible, reducing the number of possible parameters of interest.

5. Conclusions

The present study provides the first attempt to study execution and imagery of a grasping movement with a DCM-PEB approach, focusing on premotor dynamics.

On balance, we succeeded in enlightening the role of areas recently found to be involved in grasping; moreover, our model provides new evidence on the functioning of the whole grasping circuit, clarifying the ambiguous last steps of the circuit that involve PMd, PMv, and M1. This is the first attempt to analyse connectivity in the grasping network by using the DCM-PEB approach and with a surface-based ROI definition. Furthermore, differently from previous DCM studies, the evaluation of feedback connections allowed us to make inferences also on the serial activation of these areas, an information otherwise impossible to detect by using canonical fMRI analysis. Finally, the comparison between real and imagined grasping reveals that premotor areas dynamically interplay in different ways, depending on task demands.

Overall, our study suggests that disengaging from an activation perspective, where a similar recruitment of motor-related areas has been found in ME and MI, effective connectivity may provide an explanation of the substantial similarities and differences between imagined and executed grasping. Indeed, the task-dependent interactions revealed by DCM can be only partially explained by the slighter recruitment of the areas within the grasping network during MI we detected in the whole-brain activation maps (Sulpizio et al., 2020). If so, we would have found that the same connections were modulated by both conditions, but to a lesser extent during imagery. Our results suggested that this is true only for a few connections. Such findings could be useful when using MI in rehabilitation protocols of post-stroke patients (Page et al., 2007) and applied to brain computer interface (BCI) (Green and Kalaska, 2011), as well as when evaluating the effectiveness of such procedure (Doyon et al., 2003; Nyberg et al., 2006; Bajaj et al., 2015).

Further studies might extend the circuit of interest as previous functional connectivity studies (Hutchison and Gallivan, 2018) to understand whether other brain areas, excluded from our model, may account for differences in connectivity during imagined and executed grasping. It would be also useful focusing on the visual processing of the stimulus, especially for the imagined condition, or evaluating how intrahemispheric couplings are modulated by the interhemispheric connections.

Availability of data and material

Functional data used in the present study are available on Github (https://github.com/fbencive/graspingDCM_Data).

Code availability

Scripts used for data analyses are included in the SPM12 software (r7771).

Declaration of Competing Interest

We have no conflict of interest to declare.

Credit authorship contribution statement

Federica Bencivenga: Conceptualization, Methodology, Formal analysis, Visualization, Writing - original draft. **Valentina Sulpizio:** Conceptualization, Investigation, Writing - original draft. **Maria Giulia Tullo:** Methodology, Data curation, Writing - review & editing. **Gaspare Galati:** Software, Resources, Writing - review & editing, Supervision, Project administration.

Acknowledgments

The present study has been supported by funding from Sapienza University of Rome (PhD program in Behavioral Neuroscience).

Supplementary materials

Supplementary material associated with this article can be found, in the online version, at doi:10.1016/j.neuroimage.2021.117806.

References

Alexander, G.E., Crutcher, M.D., 1990. Preparation for movement: neural representations of intended direction in three motor areas of the monkey. J. Neurophysiol. 64 (1), 133–150.

Arbib, M.A., Mundhenk, T.N., 2005. Schizophrenia and the mirror system: an essay. Neuropsychologia 43 (2), 268–280. doi:10.1016/j.neuropsychologia.2004.11.013.

Ashe, J., Taira, M., Smyrnis, N., Pellizzer, G., Georgakopoulos, T., Lurito, J.T., Georgopoulos, A.P., 1993. Motor cortical activity preceding a memorized movement trajectory with an orthogonal bend. Exp. Brain Res. 95 (1), 118–130.

Bajaj, S., Butler, A.J., Drake, D., Dhamala, M., 2015. Brain effective connectivity during motor-imagery and execution following stroke and rehabilitation. NeuroImage. Clin.l 8, 572–582. doi:10.1016/j.nicl.2015.06.006.

Begliomini, C, Caria, A, Grodd, W, Castiello, U., 2007a. Comparing natural and constrained movements: new insights into the visuomotor control of grasping. PLoS One 2 (10), e1108.

Begliomini, C, Wall, MB, Smith, AT, Castiello, U., 2007b. Differential cortical activity for precision and whole-hand visually guided grasping in humans. Eur J. Neurosci. 25, 1245–1252.

Begliomini, C., Sartori, L., di Bono, M.G., Budisavljević, S., Castiello, U., 2018. The neural correlates of grasping in left-handers: When handedness does not matter. Front. Neurosci. 12, 192. doi:10.3389/fnins.2018.00192.

Begliomini, C., Sartori, L., Miotto, D., Stramare, R., Motta, R., Castiello, U., 2015. Exploring manual asymmetries during grasping: a dynamic causal modeling approach. Front. Psychol. 6, 167. doi:10.3389/fpsyg.2015.00167.

Belmalih, A., Borra, E., Contini, M., Gerbella, M., Rozzi, S., Luppino, G., 2009. Multimodal architectonic subdivision of the rostral part (area F5) of the macaque ventral premotor cortex. J. Comp. Neurol. 512 (2), 183–217. doi:10.1002/cne.21892.

Benjamini, Y., Hochberg, Y., 1995. Controlling the false discovery rate: a practical and powerful approach to multiple testing. J. R. Stat. Soc. Series B 57, 289–300.

Binkofski, F, Dohle, C, Posse, S, Stephan, KM, Hefter, H, Seitz, RJ, 1998. Human anterior intraparietal area subserves prehension: a combined lesion and functional MRI activation study. Neurology 50, 1253–1259.

Binkofski, F., Buxbaum, L.J., 2013. Two action systems in the human brain. Brain Lang. 127 (2), 222–229. doi:10.1016/j.bandl.2012.07.007.

Bozzacchi, C., Giusti, M.A., Pitzalis, S., Spinelli, D., Di Russo, F., 2012. Similar cerebral motor plans for real and virtual actions. PLoS One 7 (10), e47783. doi:10.1371/journal.pone.0047783.

Bursztyn, L.L.C.D., Ganesh, G., Imamizu, H., Kawato, M., Flanagan, J.R., 2006. Neural correlates of internal-model loading. Curr. Biol. 16 (24), 2440–2445. doi:10.1016/j.cub.2006.10.051.

Buxton, R.B., Wong, E.C., Frank, L.R., 1998. Dynamics of blood flow and oxygenation changes during brain activation: the balloon model.. Magn. Reson. Med. 39 (6), 855–864. doi:10.1002/mrm.1910390602.

Cao, Y., Hao, Y., Liao, Y., Xu, K., Wang, Y., Zhang, S., Zhang, Q., Chen, W., Zheng, X., 2013. Information analysis on neural tuning in dorsal premotor cortex for reaching and grasping. Comput. Math. Methods Med. doi:10.1155/2013/730374, 2013.

Castiello, U., Begliomini, C., 2008. The cortical control of visually guided grasping. Neuroscientist 14, 157–170. doi:10.1177/1073858407312080.

Cavina-Pratesi, C., Monaco, S., Fattori, P., Galletti, C., McAdam, T.D., Quinlan, D.J., Culham, J.C., 2010. Functional magnetic resonance imaging reveals the neural substrates of arm transport and grip formation in reach-to-grasp actions in humans. J. Neurosci. 30 (31), 10306–10323.

Choi, S.H., Na, D.L., Kang, E., Lee, K.M., Lee, S.W., Na, D.G., 2001. Functional magnetic resonance imaging during pantomiming tool-use gestures. Exp. Brain Res. 139 (3), 311–317. doi:10.1007/s002210100777.

Cona, G., Semenza, C., 2017. Supplementary motor area as key structure for domain-general sequence processing: a unified account. Neurosci. Biobehav. Rev. 72, 28–42. doi:10.1016/j.neubiorev.2016.10.033.

Culham, J., 2004. Human brain imaging reveals a parietal area specialized for grasping. In: Duncan, J, Kanwisher, N (Eds.), Attention and Performance: Functional Neuroimaging of Visual Cognition. Oxford University Press, OxfordUK, pp. 417–438.

Culham, JC, Danckert, SL, DeSouza, JF, Gati, JS, Menon, RS, Goodale, MA., 2003. Visually guided grasping produces fMRI activation in dorsal but not ventral stream brain areas. Exp Brain Res. 153, 180–189.

Dafotakis, M., Sparing, R., Eickhoff, S.B., Fink, G.R., Nowak, D.A., 2008. On the role of the ventral premotor cortex and anterior intraparietal area for predictive and reactive scaling of grip force. Brain Res. 1228, 73–80. doi:10.1016/j.brainres.2008.06.027.

Dale, A.M., Fischl, B., Sereno, M.I., 1999. Cortical surface-based analysis i. segmentation and surface reconstruction. Neuroimage 9, 179–194.

Dancause, N, Barbay, S, Frost, SB, Plautz, EJ, Popescu, M, Dixon, PM, 2006. Topographically divergent and convergent connectivity between premotor and primary motor cortex. Cereb Cortex 16 (8), 1057–1068.

Davare, M., Andres, M., Clerget, E., Thonnard, J.L., Olivier, E., 2007. Temporal dissociation between hand shaping and grip force scaling in the anterior intraparietal area. J. Neurosci. 27 (15), 3974–3980. doi:10.1523/JNEUROSCI.0426-07.2007.

Davare, M., Andres, M., Cosnard, G., Thonnard, J.L., Olivier, E., 2006. Dissociating the role of ventral and dorsal premotor cortex in precision grasping. J. Neurosci. 26 (8), 2260–2268. doi:10.1523/JNEUROSCI.3386-05.2006.

Davare, M., Kraskov, A., Rothwell, J.C., Lemon, R.N., 2011. Interactions between areas of the cortical grasping network. Curr. Opin. Neurobiol. 21, 565–570. doi:10.1016/j.conb.2011.05.021.

Desikan, R.S., Ségonne, F., Fischl, B., Quinn, B.T., Dickerson, B.C., Blacker, D., Killiany, R.J., 2006. An automated labeling system for subdividing the human cerebral cortex on MRI scans into gyral based regions of interest. Neuroimage 31 (3), 968–980. doi:10.1016/j.neuroimage.2006.01.021.

Dijkstra, N., Zeidman, P., Ondobaka, S., van Gerven, M.A.J., Friston, K., 2017. Distinct top-down and bottom-up brain connectivity during visual perception and imagery. Sci. Rep. 7 (1). doi:10.1038/s41598-017-05888-8.

Doyon, J., Penhune, V., Ungerleider, L.G., 2003. Distinct contribution of the corticostriatal and cortico-cerebellar systems to motor skill learning. Neuropsychologia 41, 252–262. doi:10.1016/S0028-3932(02)00158-6.

Dum, Strick, 1996. Spinal cord terminations of the medial wall motor areas in macaque monkeys.. Journal of Neuroscience doi:10.1523/JNEUROSCI.16-20-06513.1996.

Dum, R.P., Strick, P.L., 2005. Frontal lobe inputs to the digit representations of the motor areas on the lateral surface of the hemisphere. J. Neurosci. 25 (6), 1375–1386. doi:10.1523/JNEUROSCI.3902-04.2005.

Edelman, S., Grill-Spector, K., Kushnir, T., Malach, R., 1998. Toward direct visualization of the internal shape representation space by fMRI. Psychobiology 26, 309–321.

Fabbri, S., Stubbs, K.M., Cusack, R., Culham, J.C., 2016. Disentangling representations of object and grasp properties in the human brain. J. Neurosci. 36, 7648–7662. doi:10.1523/JNEUROSCI.0313-16.2016.

Fagg, A.H., Arbib, M.A., 1998. Modeling parietal–premotor interactions in primate control of grasping. Neural Netw. 11 (7-8), 1277–1303. doi:10.1016/S0893-6080(98)00047-1.

Faillenot, I, Toni, I, Decety, J, Gregoire, MC, Jeannerod, M, 1997. Visual pathways for object-oriented action and object recognition: functional anatomy with PET. Cereb Cortex 7 (1), 77–85.

Fischl, B., Sereno, M.I., Tootell, R.B., Dale, A.M., 1999b. High-resolution intersubject averaging and a coordinate system for the cortical surface. Hum. Brain Mapp. 8 (4), 272–284. doi:10.1002/(SICI)1097-0193(1999)8:4<272::AID-HBM10>3.0.CO;2-4.

Fischl, B., Sereno, M.I., Dale, A.M., 1999a. Cortical surface-based analysis: II. Inflation, flattening, and a surface-based coordinate system. Neuroimage 9, 195–207. http://doi.org/10.1006/nimg.1998.0396.

Flanagan, J.R., Wing, A.M., 1997. The role of internal models in motion planning and control: evidence from grip force adjustments during movements of hand-held loads. J. Neurosci. 17 (4), 1519–1528. doi:10.1523/JNEUROSCI.17-04-01519.1997.

Fogassi, L., Gallese, V., Buccino, G., Craighero, L., Fadiga, L., Rizzolatti, G., 2001. Cortical mechanism for the visual guidance of hand grasping movements in the monkey A reversible inactivation study. Brain 124 (3), 571–586.

Frey, SH, Vinton, D, Norlund, R, Grafton, ST., 2005. Cortical topography of human anterior intraparietal cortex active during visually guided grasping. Brain Res. Cogn. Brain Res. 23 (2-3), 397–405.

Friston, K.J., Harrison, L., Penny, W., 2003. Dynamic causal modelling. Neuroimage 19 (4), 1273–1302. doi:10.1016/S1053-8119(03)00202-7.

Friston, K.J., Kahan, J., Biswal, B., Razi, A., 2014. A DCM for resting state fMRI. Neuroimage 94, 396–407. doi:10.1016/j.neuroimage.2013.12.009.

Friston, K.J., Litvak, V., Oswal, A., Razi, A., Stephan, K.E., Van Wijk, B.C., Zeidman, P., 2016. Bayesian model reduction and empirical Bayes for group (DCM) studies. Neuroimage 128, 413–431. doi:10.1016/j.neuroimage.2015.11.015.

Friston, K.J., Mechelli, A., Turner, R., Price, C.J., 2000. Nonlinear responses in fMRI: the Balloon model, Volterra kernels, and other hemodynamics. Neuroimage 12 (4), 466–477. doi:10.1006/nimg.2000.0630.

Friston, K., Penny, W., 2011. Post hoc Bayesian model selection. Neuroimage 56 (4), 2089–2099. doi:10.1016/j.neuroimage.2011.03.062.

Friston, K., Chu, C., Mourão-Miranda, J., Hulme, O., Rees, G., Penny, W., Ashburner, J., 2008. Bayesian decoding of brain images. Neuroimage 39, 181–205.

Friston, K., Mattout, J., Trujillo-Barreto, N., Ashburner, J., Penny, W., 2007. Variational free energy and the Laplace approximation. Neuroimage 34 (1), 220–234. doi:10.1016/J.NEUROIMAGE.2006.08.035.

Friston, K., Zeidman, P., Litvak, V., 2015. Empirical Bayes for DCM: a group inversion scheme.. Front. Syst. Neurosci. 9, 164. doi:10.3389/fnsys.2015.00164.

Galati, G., Committeri, G., Spitoni, G., Aprile, T., Di Russo, F., Pitzalis, S., Pizzamiglio, L., 2008. A selective representation of the meaning of actions in the auditory mirror system. Neuroimage 40, 1274–1286. doi:10.1016/j.neuroimage.2007.12.044.

Gallivan, J.P., McLean, D.A., Flanagan, J.R., Culham, J.C., 2013. Where one hand meets the other: limb-specific and action-dependent movement plans decoded from preparatory signals in single human frontoparietal brain areas. J. Neurosci. 33, 1991–2008. doi:10.1523/JNEUROSCI.0541-12.2013.

Gallivan, J.P., McLean, D.A., Smith, F.W., Culham, J.C., 2011a. Decoding effector-dependent and effector-independent movement intentions from human parieto-frontal brain activity. J. Neurosci. 31, 17149–17168. doi:10.1523/JNEUROSCI.1058-11.2011.

Gallivan, J.P., McLean, D.A., Valyear, K.F., Pettypiece, C.E., Culham, J.C., 2011b. Decoding action intentions from preparatory brain activity in human parieto-frontal networks. J. Neurosci. 31, 9599–9610. doi:10.1523/JNEUROSCI.0080-11.2011.

Gao, Q, Duan, X, Chen, H., 2011. Evaluation of effective connectivity of motor areas during motor imagery and execution using conditional Granger causality. Neuroimage 54 (2), 1280–1288.

Gao, Q., Tao, Z., Zhang, M., Chen, H., 2014. Differential contribution of bilateral supplementary motor area to the effective connectivity networks induced by task conditions using dynamic causal modeling. Brain Connect. 4 (4), 256–264. doi:10.1089/brain.2013.0194.

Georgopoulos, A.P., Grillner, S., 1989. Visuomotor coordination in reaching and locomotion. Science 245 (4923), 1209–1210.

Gerbella, M., Belmalih, A., Borra, E., Rozzi, S., Luppino, G., 2011. Cortical connections of the anterior (F5a) subdivision of the macaque ventral premotor area F5. Brain Struct. Funct. 216 (1), 43–65. doi:10.1007/s00429-010-0293-6.

Gerbella, M., Rozzi, S., Rizzolatti, G., 2017. The extended object-grasping network. Exp. Brain Res. 235, 2903–2916. doi:10.1007/s00221-017-5007-3.

Glasser, M.F., Sotiropoulos, S.N., Wilson, J.A., Coalson, T.S., Fischl, B., Andersson, J.L., Van Essen, D.C., 2013. The minimal preprocessing pipelines for the human connectome project. Neuroimage 80, 105–124. http://doi.org/10.1016/j.neuroimage.2013.04.127.

Godschalk, M, Lemon, RN, Kuypers, HG, Ronday, HK., 1984. Cortical afferents and efferents of monkey postarcuate area: an anatomical and electrophysiological study. Exp Brain Res. 56 (3), 410–424.

Goldberg, G., 1985. Supplementary motor area structure and function: Review and hypotheses. Behav. Brain Sci. 8 (4), 567–588. doi:10.1017/S0140525X00045167.

Grafton, ST, Arbib, MA, Fadiga, L, Rizzolatti, G., 1996. Localization of grasp representations in humans by positron emission tomography. 2. Observation compared with imagination. Exp Brain Res. 112, 103–111.

Green, A.M., Kalaska, J.F., 2011. Learning to move machines with the mind. Trends Neurosci. 34, 61–75. doi:10.1016/j.tins.2010.11.003.

Grol, M.J., Majdandžić, J., Stephan, K.E., Verhagen, L., Dijkerman, H.C., Bekkering, H., Toni, I., 2007. Parieto-frontal connectivity during visually guided grasping. J. Neurosci. 27 (44), 11877–11887. doi:10.1523/JNEUROSCI.3923-07.2007.

Guillot, A., Collet, C., Nguyen, V.A., Malouin, F., Richards, C., Doyon, J., 2009. Brain activity during visual versus kinesthetic imagery: an fMRI study. Hum. Brain Mapp. 30 (7), 2157–2172. doi:10.1002/hbm.20658.

Haller, S., Chapuis, D., Gassert, R., Burdet, E., Klarhöfer, M., 2009. Supplementary motor area and anterior intraparietal area integrate fine-graded timing and force control during precision grip. Eur. J. Neurosci. 30 (12), 2401–2406. doi:10.1111/j.1460-9568.2009.07003.x.

Halsband, U., Ito, N., Tanji, J., Freund, H.J., 1993. The role of premotor cortex and the supplementary motor area in the temporal control of movement in man. Brain 116 (1), 243–266. doi:10.1093/brain/116.1.243.

Hamilton, A.F.D.C., Grafton, S.T., 2006. Goal representation in human anterior intraparietal sulcus. J. Neurosci. 26 (4), 1133–1137. doi:10.1523/JNEUROSCI.4551-05.2006.

Hardwick, R.M., Caspers, S., Eickhoff, S.B., Swinnen, S.P., 2018. Neural correlates of action: Comparing meta-analyses of imagery, observation, and execution. Neurosci. Biobehav. Rev. 94, 31–44. doi:10.1016/j.neubiorev.2018.08.003.

Haxby, J.V., Gobbini, M.I., Furey, M.L., Ishai, A., Schouten, J.L., Pietrini, P., 2001. Distributed and overlapping representations of faces and objects in ventral temporal cortex. Science 293, 2425–2430.

He, S.Q., Dum, R.P., Strick, P.L., 1993. Topographic organization of corticospinal projections from the frontal lobe: motor areas on the lateral surface of the hemisphere. J. Neurosci. 13 (3), 952–980. doi:10.1523/JNEUROSCI.13-03-00952.1993.

Hermsdörfer, J., Terlinden, G., Mühlau, M., Goldenberg, G., Wohlschläger, A.M., 2007. Neural representations of pantomimed and actual tool use: evidence from an event-related fMRI study. Neuroimage 36, T109–T118.

Hètu, S., Grégoire, M., Saimpont, A., Coll, M.P., Eugène, F., Michon, P.E., Jackson, P.L., 2013. The neural network of motor imagery: an ALE meta-analysis. Neurosci. Biobehav. Rev. 37 (5), 930–949. doi:10.1016/j.neubiorev.2013.03.017.

Hoeting, J.A., Madigan, D., Raftery, A.E., Volinsky, C.T., 1999. Bayesian model averaging: a tutorial. Stat. Sci. 382–401.

Hoshi, E., Tanji, J., 2007. Distinctions between dorsal and ventral premotor areas: anatomical connectivity and functional properties. Curr. Opin. Neurobiol. 17 (2), 234–242.

Huber, L., Handwerker, D.A., Jangraw, D.C., Chen, G., Hall, A., Stuber, C., Gonzalez–Castillo, J., Ivanov, D., Marrett, S., Guidi, M., et al., 2017. High resolution CBV-fMRI allows mapping of laminar activity and connectivity of cortical input and output in human M1. Neuron 96, 1253–1263.

Huber, L., Ivanov, D., Handwerker, D.A., Marrett, S., Guidi, M., Uludag, K., Bandettini, P.A., Poser, B.A., 2018. Techniques for blood volume fMRI with VASO: from low-resolution mapping towards sub-millimeter layer-dependent applications. Neuroimage 164, 131–143.

Hutchison, R.M., Gallivan, J.P., 2018. Functional coupling between frontoparietal and occipitotemporal pathways during action and perception. Cortex 98, 8–27. doi:10.1016/j.cortex.2016.10.020.

Jeannerod, M., Arbib, M.A., Rizzolatti, G., Sakata, H., 1995. Grasping objects: the cortical mechanisms of visuomotor transformation. Trends Neurosci. 18, 314–320.

Jiang, D., Edwards, M.G., Mullins, P., Callow, N., 2015. The neural substrates for the different modalities of movement imagery. Brain Cogn. 97, 22–31. doi:10.1016/j.bandc.2015.04.005.

Johansson, R.S., Westling, G., 1984. Roles of glabrous skin receptors and sensorimotor memory in automatic control of precision grip when lifting rougher or more slippery objects. Exp. Brain Res. 56 (3), 550–564. doi:10.1007/BF00237997.

Johansson, R.S., Westling, G., 1988. Coordinated isometric muscle commands adequately and erroneously programmed for the weight during lifting task with precision grip. Exp. Brain Res. 71 (1), 59–71. doi:10.1007/BF00247522.

Johnson-Frey, S.H., Newman-Norlund, R., Grafton, S.T., 2005. A distributed left hemisphere network active during planning of everyday tool use skills. Cereb. Cortex 15, 681–695. doi:10.1093/cercor/bhh169.

Kalaska, J.F., Crammond, D.J., 1992. Cerebral cortical mechanisms of reaching movements. Science 255 (5051), 1517–1523.

Kasess, C.H., Windischberger, C., Cunnington, R., Lanzenberger, R., Pezawas, L., Moser, E., 2008. The suppressive influence of SMA on M1 in motor imagery revealed by fMRI and dynamic causal modeling. Neuroimage 40 (2), 828–837. doi:10.1016/J.NEUROIMAGE.2007.11.040.

Króliczak, G., Cavina-Pratesi, C., Goodman, D.A., Culham, J.C., 2007. What does the brain do when you fake it? An FMRI study of pantomimed and real grasping. J. Neurophysiol. 97 (3), 2410–2422. doi:10.1152/jn.00778.2006.

Kuhtz-Buschbeck, J.P., Ehrsson, H.H., Forssberg, H., 2001. Human brain activity in the control of fine static precision grip forces: an fMRI study. Eur. J. Neurosci. 14 (2), 382–390. doi:10.1046/j.0953-816X.2001.01639.x.

Kwong, K.K., Belliveau, J.W., Chesler, D.A., Goldberg, I.E., Weisskoff, R.M., Poncelet, B.P., Kennedy, D.N., Hoppel, B.E., Cohen, M.S., Turner, R., 1992. Dynamic magnetic resonance imaging of human brain activity during primary sensory stimulation. Proc. Natl. Acad. Sci. U.S.A. 89, 5675–5679.

Maier, M.A., Armand, J., Kirkwood, P.A., Yang, H.W., Davis, J.N., Lemon, R.N., 2002. Differences in the corticospinal projection from primary motor cortex and supplementary motor area to macaque upper limb motoneurons: an anatomical and electrophysiological study. Cereb. Cortex 12 (3), 281–296. doi:10.1093/cercor/12.3.281.

Makuuchi, M., Someya, Y., Ogawa, S., Takayama, Y., 2012. Hand shape selection in pantomimed grasping: interaction between the dorsal and the ventral visual streams and convergence on the ventral premotor area. Hum. Brain Mapp. 33 (8), 1821–1833. doi:10.1002/hbm.21323.

Mangan, A.P., Whitaker, R.T., 1999. Partitioning 3D surface meshes using watershed segmentation. IEEE Trans. Vis. Comput. Graph. 5 (4), 308–321.

Mao, T., Kusefoglu, D., Hooks, B.M., Huber, D., Petreanu, L., Svoboda, K., 2011. Long-range neuronal circuits underlying the interaction between sensory and motor cortex. Neuron 72, 111–123.

Marconi, B., Genovesio, A., Battaglia-Mayer, A., Ferraina, S., Squatrito, S., Molinari, M., Caminiti, R., 2001. Eye–hand coordination during reaching. I. Anatomical relationships between parietal and frontal cortex. Cereb. Cortex 11 (6), 513–527. doi:10.1093/cercor/11.6.513.

Martino, A.M., Strick, P.L., 1987. Corticospinal projections originate from the arcuate premotor area. Brain Res. 404 (1-2), 307–312. doi:10.1016/0006-8993(87)91384-9.

Matelli, M, Camarda, R, Glickstein, M, Rizzolatti, G., 1986. Afferent and efferent projections of the inferior area 6 in the macaque monkey. J. Comp. Neurol. 251, 281–298.

Monaco, S., Malfatti, G., Culham, J.C., Cattaneo, L., Turella, L., 2020. Decoding motor imagery and action planning in the early visual cortex: Overlapping but distinct neural mechanisms. Neuroimage 218, 116981. doi:10.1016/j.neuroimage.2020.116981.

Monaco, S., Sedda, A., Cavina-Pratesi, C., Culham, J.C., 2015. Neural correlates of object size and object location during grasping actions. Eur. J. Neurosci. 41 (4), 454–465. doi:10.1111/ejn.12786.

Muakkassa, KF, Strick, PL., 1979. Frontal lobe inputs to primate motor cortex: evidence for four somatotopically organized 'premotor' areas. Brain Res 177, 176–182.

Murata, A., Gallese, V., Luppino, G., Kaseda, M., Sakata, H., 2000. Selectivity for the shape, size, and orientation of objects for grasping in neurons of monkey parietal area AIP. J. Neurophysiol. 83 (5), 2580–2601.

Nowak, D.A., Berner, J., Herrnberger, B., Kammer, T., Grön, G., Schönfeldt-Lecuona, C., 2009. Continuous theta-burst stimulation over the dorsal premotor cortex interferes with associative learning during object lifting. Cortex 45 (4), 473–482. doi:10.1016/j.cortex.2007.11.010.

Nyberg, L., Eriksson, J., Larsson, A., Marklund, P., 2006. Learning by doing versus learning by thinking: an fMRI study of motor and mental training. Neuropsychologia 44, 711–717. doi:10.1016/j.neuropsychologia.2005.08.006.

Oldfield, R.C., 1971. The assessment and analysis of handedness: the Edinburgh inventory. Neuropsychologia 9, 97–113. doi:10.1016/0028-3932(71)90067-4.

Olivier, E., Davare, M., Andres, M., Fadiga, L., 2007. Precision grasping in humans: from motor control to cognition. Curr. Opin. Neurobiol. 17, 644–648. doi:10.1016/j.conb.2008.01.008.

Orgogozo, J.M., Larsen, B., 1979. Activation of the supplementary motor area during voluntary movement in man suggests it works as a supramotor area. Science 206 (4420), 847–850. doi:10.1126/science.493986.

Page, S.J., Levine, P., Leonard, A., 2007. Mental practice in chronic stroke: results of a randomized, placebo-controlled trial. Stroke 38, 1293–1297. doi:10.1161/01.STR.0000260205.67348.2b.

Papitto, G., Friederici, A.D., Zaccarella, E., 2020. The topographical organization of motor processing: an ALE meta-analysis on six action domains and the relevance of Broca's region. Neuroimage 206, 116321. doi:10.1016/j.neuroimage.2019.116321.

Park, C.H., Chang, W.H., Lee, M., Kwon, G.H., Kim, L., Kim, S.T., Kim, Y.H., 2015. Which motor cortical region best predicts imagined movement? Neuroimage 113, 101–110.

Penny, W., Mattout, J., Trujillo-Barreto, N., 2006. Bayesian model selection and averaging.. Statistical Parametric Mapping: The Analysis of Functional Brain Images. Elsevier, London.

Persichetti, A.S., Avery, J.A., Huber, L., Merriam, E.P., Martin, A., 2020. Layer-specific contributions to imagined and executed hand movements in human primary motor cortex. Curr. Biol. 30, 1721–1725. doi:10.1016/j.cub.2020.02.046, e3.

Picard, N., Strick, P.L., 2003. Activation of the supplementary motor area (SMA) during performance of visually guided movements. Cereb. Cortex 13 (9), 977–986. doi:10.1093/cercor/13.9.977.

Pilgramm, S., de Haas, B., Helm, F., Zentgraf, K., Stark, R., Munzert, J., Krüger, B., 2016. Motor imagery of hand actions: decoding the content of motor imagery from brain activity in frontal and parietal motor areas. Hum. Brain Mapp. 37, 81–93. doi:10.1002/hbm.23015.

Pinotsis, D.A., Perry, G., Litvak, V., Singh, K.D., Friston, K.J., 2016. Intersubject variability and induced gamma in the visual cortex: DCM with empirical Bayes and neural fields. Hum. Brain Mapp. 37 (12), 4597–4614. doi:10.1002/hbm.23331.

Power, J.D., Barnes, K.A., Snyder, A.Z., Schlaggar, B.L., Petersen, S.E., 2012. Spurious but systematic correlations in functional connectivity MRI networks arise from subject motion. Neuroimage 59 (3), 2142–2154. doi:10.1016/j.neuroimage.2011.10.018.

Raos, V., Umiltá, M.A., Gallese, V., Fogassi, L., 2004. Functional properties of grasping-related neurons in the dorsal premotor area F2 of the macaque monkey. J. Neurophysiol. 92 (4), 1990–2002. doi:10.1152/jn.00154.2004.

Rizzolatti, G., Luppino, G., 2001. The cortical motor system. Neuron 31 (6), 889–901. doi:10.1016/S0896-6273(01)00423-8.

Rizzolatti, G., Luppino, G., Matelli, M., 1998. The organization of the cortical motor system: new concepts. Electroencephalogr. Clin. Neurophysiol. 106 (4), 283–296.

Roland, P.E., Larsen, B., Lassen, N.A., Skinhoj, E., 1980. Supplementary motor area and other cortical areas in organization of voluntary movements in man. J. Neurophysiol. 43 (1), 118–136. doi:10.1152/jn.1980.43.1.118.

Rosa, M.J., Friston, K., Penny, W., 2012. Post-hoc selection of dynamic causal models. J. Neurosci. Methods 208 (1), 66–78. doi:10.1016/J.JNEUMETH.2012.04.013.

Rushworth, M.F., Nixon, P.D., Wade, D.T., Renowden, S., Passingham, R.E., 1998. The left hemisphere and the selection of learned actions. Neuropsychologia 36 (1), 11–24. doi:10.1016/S0028-3932(97)00101-2.

Sakata, H., Taira, M., Murata, A., Mine, S., 1995. Neural mechanisms of visual guidance of hand action in the parietal cortex of the monkey. Cereb. Cortex 5 (5), 429–438.

Schaffelhofer, S., Scherberger, H., 2016. Object vision to hand action in macaque parietal, premotor, and motor cortices. Elife 5, e15278. doi:10.7554/eLife.15278.001.

Seki, K, Fetz, EE., 2012. Gating of sensory input at spinal and cortical levels during preparation and execution of voluntary movement. J. Neurosci. 32, 890–902.

Sharma, S., Mantini, D., Vanduffel, W., Nelissen, K., 2019. Functional specialization of macaque premotor F5 subfields with respect to hand and mouth movements: a comparison of task and resting-state fMRI. Neuroimage 191, 441–456. doi:10.1016/j.neuroimage.2019.02.045.

Shikata, E., Hamzei, F., Glauche, V., Koch, M., Weiller, C., Binkofski, F., Buchel, C., 2003. Functional properties and interaction of the anterior and posterior intraparietal areas in humans. Eur. J. Neurosci. 17, 1105–1110. doi:10.1046/j.1460-9568.2003.02540.x.

Shimazu, H., Maier, M.A., Cerri, G., Kirkwood, P.A., Lemon, R.N., 2004. Macaque ventral premotor cortex exerts powerful facilitation of motor cortex outputs to upper limb motoneurons. J. Neurosci. 24 (5), 1200–1211. doi:10.1523/JNEUROSCI.4731-03.2004.

Simon, O., Mangin, J.F., Cohen, L., Le Bihan, D., Dehaene, S., 2002. Topographical layout of hand, eye, calculation, and language-related areas in the human parietal lobe. Neuron 33, 475–487.

Smith, A.M., Bourbonnais, D., Blanchette, G., 1981. Interaction between forced grasping and a learned precision grip after ablation of the supplementary motor area. Brain Res. 222 (2), 395–400. doi:10.1016/0006-8993(81)91043-X.

Solodkin, A, Hlustik, P, Chen, EE, Small, SL., 2004. Fine modulation in network activation during motor execution and motor imagery. Cereb Cortex 14, 1246–1255.

Stephan, K.E., Penny, W.D., Moran, R.J., den Ouden, H.E., Daunizeau, J., Friston, K.J., 2010. Ten simple rules for dynamic causal modeling. Neuroimage 49 (4), 3099–3109.

Sulpizio, V., Neri, A., Fattori, P., Galletti, C., Pitzalis, S., Galati, G., 2020. Real and imagined grasping movements differently activate the human dorsomedial parietal cortex. Neuroscience 434, 22–34. doi:10.1016/J.NEUROSCIENCE.2020.03.019.

Sun, H., Blakely, T.M., Darvas, F., Wander, J.D., Johnson, L.A., Su, D.K., Ojemann, J.G., 2015. Sequential activation of premotor, primary somatosensory and primary motor areas in humans during cued finger movements. Clin. Neurophysiol. 126 (11), 2150–2161. doi:10.1016/j.clinph.2015.01.005.

Taira, M., Mine, S., Georgopoulos, A.P., Murata, A., Sakata, H., 1990. Parietal cortex neurons of the monkey related to the visual guidance of hand movement. Exp. Brain Res. 83 (1), 29–36. doi:10.1007/BF00232190.

Trampel, R., Bazin, P.L., Pine, K., Weiskopf, N., 2019. In-vivo magnetic resonance imaging (MRI) of laminae in the human cortex. Neuroimage 197, 707–715.

Tunik, E, Rice, NJ, Hamilton, A, Grafton, ST., 2007. Beyond grasping: representation of action in human anterior intraparietal sulcus. Neuroimage 36, T77–T86. doi:10.1016/j.neuroimage.2007.03.026.

Turella, L., Rumiati, R., Lingnau, A., 2020. Hierarchical action encoding within the human brain. Cereb. Cortex 30, 2924–2938. doi:10.1093/cercor/bhz284.

Turner, R., 2016. Uses, misuses, new uses and fundamental limitations of magnetic resonance imaging in cognitive science. Philos. Trans. R. Soc. Lond. B Biol. Sci. 371, 20150349.

Van Essen, D.C., Glasser, M.F., Dierker, D.L., Harwell, J., Coalson, T., 2012. Parcellations and hemispheric asymmetries of human cerebral cortex analyzed on surface-based atlases. Cereb. Cortex 22, 2241–2262. doi:10.1093/cercor/bhr291.

Weiler, N., Wood, L., Yu, J., Solla, S.A., Shepherd, G.M., 2008. Topdown laminar organization of the excitatory network in motor cortex. Nat. Neurosci. 11, 360–366.

White, O., Davare, M., Andres, M., Olivier, E., 2013. The role of left supplementary motor area in grip force scaling. PLoS One 8 (12), e83812. doi:10.1371/journal.pone.0083812.

Yousry, T.A., Schmid, U.D., Alkadhi, H., Schmidt, D., Peraud, A., Buettner, A., Winkler, P., 1997. Localization of the motor hand area to a knob on the precentral gyrus. A new landmark. Brain 120 (1), 141–157. doi:10.1093/brain/120.1.141.

Zabicki, A., De Haas, B., Zentgraf, K., Stark, R., Munzert, J., Krüger, B., 2017. Imagined and executed actions in the human motor system: testing neural similarity between execution and imagery of actions with a multivariate approach. Cereb. Cortex 27, 4523–4536. doi:10.1093/cercor/bhw257.

Zeidman, P., Jafarian, A., Corbin, N., Seghier, M.L., Razi, A., Price, C.J., Friston, K.J., 2019a. A guide to group effective connectivity analysis, part 1: First level analysis with DCM for fMRI. Neuroimage 200, 174–190. doi:10.1016/j.neuroimage.2019.06.031.

Zeidman, P., Jafarian, A., Seghier, M.L., Litvak, V., Cagnan, H., Price, C.J., Friston, K.J., 2019b. A guide to group effective connectivity analysis, part 2: second level analysis with PEB. Neuroimage 200, 12–25. doi:10.1016/j.neuroimage.2019.06.032.